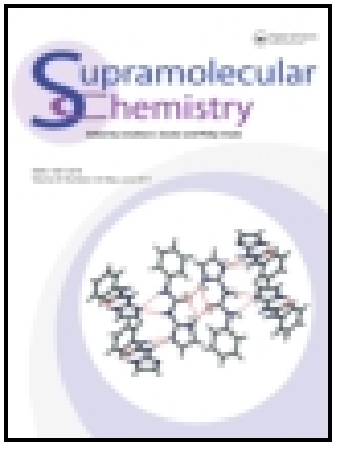

Supramolecular Chemistry
Publication details, including instructions for authors and subscription information:
http://www.tandfonline.com/loi/gsch20

Coumarin synthesis on π-acidic surfaces

François N. Miros[a], Guangxi Huang[a], Yingjie Zhao[a], Naomi Sakai[a] & Stefan Matile[a]
[a] Department of Organic Chemistry, University of Geneva, Geneva, Switzerland
Published online: 24 Sep 2014.

Supramolecular Chemistry, 2014
http://dx.doi.org/10.1080/10610278.2014.959013

Taylor & Francis
Taylor & Francis Group

Coumarin synthesis on π-acidic surfaces

François N. Miros, Guangxi Huang, Yingjie Zhao, Naomi Sakai and Stefan Matile*

Department of Organic Chemistry, University of Geneva, Geneva, Switzerland

(*Received 13 June 2014; accepted 17 August 2014*)

Catalysis with anion–π interactions is emerging as an important topic in supramolecular chemistry. Among the reactions explored so far on π-acidic surfaces, coumarin synthesis stands out as a cascade process with several coupled anionic transition states. Increasing π-acidity has been shown in a different context to increase transition-state stabilisation and thus catalytic activity. In this report, we explore the possible use of macrocycles to accelerate coumarin synthesis between two π-acidic surfaces. To our disappointment, we found that compared to monomeric π-acids, coumarin synthesis within divalent macrocycles is clearly slower. Hindered access to an overly confined active site within the macrocycles could possibly account for this loss in activity, but several other explanations are certainly possible. However, operational coumarin synthesis on monomeric π-acidic surfaces is shown to tolerate structural modifications. Best results are obtained with structures that aim for proximity without obstructing transition-state stabilisation on the π-acidic surface.

Keywords: anion–π interactions; catalysis; anionic transition states; enolates; naphthalenediimides; macrocycles

Introduction

The idea to accelerate reactions with anionic transition states on the π-acidic surfaces is intriguing because it is essentially unexplored (*1–3*). The complementary cation–π interactions have been brought to scientific attention in the late 1980s and early 1990s, mainly by work from the Dougherty group (*4*). Today, cation–π interactions are established as a central force to control interactions between and within molecules (*5*). They are routinely evoked together with hydrogen bonds, ion pairing, hydrophobic contacts and π–π interactions, and numerous examples have accumulated to testify for their central role in chemistry and biology. The importance of cation–π interactions in catalysis is best understood in the context of the biosynthesis of terpenoid natural products (*6*). Particularly impressive is the extended π-basic surface that stabilises the multiple carbocation intermediates during the enzymatic cascade cyclisation of terpenes into steroids. In chemistry, the introduction of cation–π interactions to stabilise cationic transition states has been comparably slow despite early evidence from π-basic macrocycles that the possibility exists (*4*). Today, catalysis with cation–π interactions is receiving increased attention. Examples for carbocation-based cascade cyclisation similar to steroid biosynthesis have been reported (*7*) as well as the stabilisation of several iminium, pyridinium, imidazolium and thiazolium intermediates in organocatalysis (*8*).

Consistent with their counterintuitive nature, anion–π interactions are much younger than cation–π interactions. Their existence has been explicitly proposed first in 2002 in a series of computational studies (*9–11*). For anion–π interactions to occur, electrons have to be moved from the aromatic core to the periphery until the axial quadrupole moment Q_{zz} inverts (*9–35*). This is possible with electron-withdrawing substituents, which at the same time expose the nuclear charge of the ring and introduce strong local dipole moments in the aromatic plane that could further support the binding of anions above and below this plane (Figure 1). The best-known π-acid arguably is hexafluorobenzene with $Q_{zz} = +9.0$ B (for Buckinghams) as compared to $Q_{zz} = -8.5$ B for benzene. With possible contributions from many parameters (Q_{zz} quadrupole moments, local in-plane dipoles, polarisability, π* orbitals, σ orbitals, nuclei) and other overlapping processes (in-plane C—H bonding, charge transfer, electron transfer), nature and boundaries of the attraction of anions to the surface of electron-deficient aromatic planes remain vividly debated in the community (*13–20*).

It was not trivial to secure direct experimental support for the functional relevance of anion–π interactions, to literally 'catch them at work'. Contributions of anion–π interactions to the binding (*25–34*) and transport of anions across lipid bilayer membranes (*33–35*) were obtained first. These examples for anion stabilisation in the ground state implied that anion–π interactions should also stabilise anionic transition states and reactive intermediates (*34*). The first explicit example for catalysis with anion–π interactions was reported last year, focusing on the Kemp elimination as a classical tool to elaborate on

*Corresponding author. Email: stefan.matile@chiorg.unige.ch

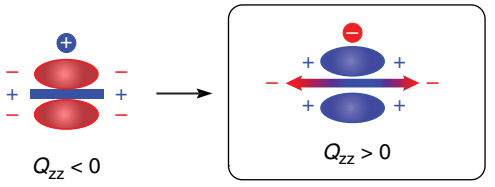

Figure 1. (Colour online) Cation–π interactions occur in electron-rich aromatic surfaces with negative Q_{zz} component of quadrupole moment (left). Anion–π interactions occur on electron-deficient aromatic planes with positive Q_{zz}, supportive local in-plane dipoles from electron-withdrawing substituents and exposed nuclear charges of the ring (right). The precise origins and boundaries of anion–π interactions are under debate.

innovative systems, including theozymes, abzymes, synzymes, etc. (*1*, *2*). Increasing transition-state stabilisation with increasing π-acidity of the catalyst provided meaningful support for the existence of operational anion–π interactions, and computational simulations were in agreement with this interpretation (*1*, *2*).

Arguably the most important anionic reactive intermediate in chemistry and biology is the enolate anion (*36–42*). In biology, enolate chemistry is most impressive in the biosynthesis of polyketide natural products, reaching from fatty acids and lipids to structures as complex and as important as the epothilones, erythromycins, amphotericins, prostaglandins or taxol (*36–40*). With the complementary cation–π interactions playing a central role in stabilising carbocation intermediates during the biosynthesis of terpenes and steroids (*6*), it was thus most intriguing to explore enolate chemistry with anion–π interactions. Placed covalently on top of an unoptimised π-acidic surface, the acidity of malonate diesters increased by $\Delta pK_a = 1.9$ (*3*). This demonstrated that the already unoptimised anion–π interactions stabilise reactive enolate intermediates by $\Delta\Delta G_{RI} = 4.7\,kJ\,mol^{-1}$. From the stabilisation of this central intermediate, the addition of the enolate to enones and nitroolefines could be accelerated significantly. Stabilisations of their anionic transition states ranged from $\Delta\Delta G_{TS} = 6.2\,kJ\,mol^{-1}$ to $\Delta\Delta G_{TS} = 11.0\,kJ\,mol^{-1}$. In this report, we elaborate on anionic cascade processes (*3*) and show that they can accelerate when placed most closely to a fully accessible π-acidic surface but decelerate when they take place sandwiched between two π-acidic surfaces within a macrocycle.

Results and discussion

Coumarins are natural products from the shikimate pathway. They are most appreciated as multipurpose fluorescent probes and laser dyes. Their sweet flavour has been used in perfumes, whereas their bitter taste might serve plants for self-defence. The synthesis of coumarin **1** is a classic in organic chemistry (Scheme 1). Resorcylaldehyde **2** and acetoacetate **3** are the substrates, the catalyst is a base, usually piperidine. This coumarin synthesis was attractive to expand enolate chemistry with anion–π interactions to cascade processes. Consider the general compound **4** with an acetoacetate substrate placed covalently on the π-acidic surface of a naphthalenediimide (NDI) (*1–3*). Addition of the base catalyst should yield enolate **5** of acetoacetate stabilised on the π-acidic surface. The stabilisation of enolate intermediates on unoptimised NDI surfaces has been confirmed experimentally to occur with a $\Delta pK_a = 1.9$, corresponding to $\Delta\Delta G_{RI} = 4.7\,kJ\,mol^{-1}$ (*3*). This enolate intermediate **5** could then attack substrate **2**. In the anionic transition state **6** of this aldol condensation, the negative charge is flowing over the π-acidic surface from the enolate to the phenolate in **7**. Driven by increasing conjugation and, perhaps, anion–π activation of the anionic leaving group, the Knoevenagel condensation is then completed with an elimination of water. In the resulting enone **8**, the phenolate is perfectly positioned to initiate the intramolecular transesterification leading to coumarin **1**. In this substitution reaction on a carbonyl group, the π-acidic surface could help either by stabilising the classical anionic tetrahedral intermediate in **9**, or by activating the unfavourable alcoholate leaving group. In principle, the released diol **10** could be reloaded *in situ* with another acetoacetate to close the catalytic cycle. However, the specific objective at this point was to explore the stabilisation of anionic transition states by anion–π interactions rather than to achieve turnover. For this purpose, the positioning of the π-acidic surface as covalent auxiliary is advantageous to minimise ambiguities.

Several aspects of the mechanism of the cascade process leading to coumarins can be discussed. For example, the piperidine base could form enamines with acetoacetate **4** or iminium cations with formaldehyde **2**. Knoevenagel condensations are expected to pass through activated iminium acceptors. However, intramolecular hydrogen bonding in resorcylaldehyde substrate **2** is presumably sufficient to activate the aromatic aldehyde for aldol condensation with the anion–π stabilised enolate in **6**. Successful coumarin synthesis with triethylamine instead of piperidine as base catalyst suggested that iminium activation is not essential.

Throughout the entire cascade process, anion–π interactions should be supported by π–π interactions. This begins with the delocalisation of the negative charge over two carbonyl groups in the enolate intermediate **5** and culminates with extended phenolate intermediate **8**, leading to the intramolecular transesterification **9**. π–π enhanced anion–π interactions and delocalised anions have been described previously in the context of nitrate–π interactions (*29*, *33*, *34*). In transition states, anions are by definition delocalised. Applied to catalysis, the concept of

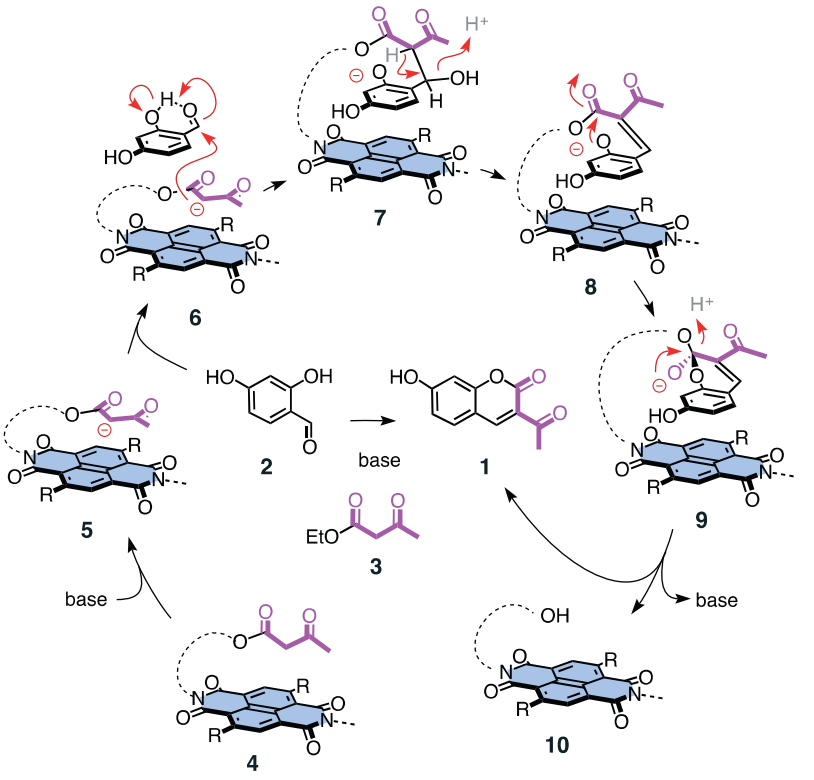

Scheme 1. (Colour online) The synthesis of coumarin **1** on a π-acidic surface. To stabilise anionic transitions states with anion–π interactions, an NDI is covalently attached to acetoacetate **3**. Deprotonation of conjugate **4** produces enolate anion of the π-acidic surface in the reactive intermediate **5**, which attacks aldehyde **2** to give the phenolate on the π-acidic surface of **7**. Dehydration of aldol **7** is followed by transesterification of the Knoevenagel product **8** with tetrahedral anionic intermediates and activates anionic leaving groups on the π-acidic surface of **9**.

anion–π interactions will thus necessarily have to evolve, presumably following the development cation–π interactions have made over the past two decades (*5*, *7*, *8*).

The acceleration of coumarin synthesis with anion–π interactions was originally explored with acetoacetate–NDI conjugate **11** (Figure 2). A rate of enhancement of $k_{rel} = k_{app}$ (**11**)/k_{app} (**3**) = 8.0 was observed (Table 1). This increase in activity corresponded to a transition-state stabilisation of $\Delta\Delta G_{TS} = 5.2\,kJ\,mol^{-1}$ by anion–π interactions (*3*). This initial experimental support for the stabilisation of an anionic cascade process on π-acidic surfaces called for confirmation and encouraged further development. For this purpose, we here report design, synthesis and evaluation of anion–π substrates **12** and **13** (Figure 2).

Compared to the original anion–π substrate **11**, the linker between acetoacetate and NDI in the new anion–π substrate **12** is shortened by two atoms to afford a preorganised '*pseudo*'-Leonard linker (*2*). This compact positioning of the acetoacetate was expected to liberate more space for the anions on the π-acidic surface during the cascade transformation of the acetoacetate in **12** into coumarin **1**, and to increase transition-state stabilisation by preorganised anion–π interactions. In macrocycle **13**, the acetoacetate substrate is sandwiched between two NDIs. This substrate inclusion was expected to maximise the stabilisation of the anionic transition states by doubled anion–π interactions.

Anion–π substrate **12** was synthesised from naphthalenedianhydride **14** (Scheme 2). Reaction with amine **15** afforded a mixture of *anti*-atropisomer **16** and *syn*-atropisomer **17**. With rotational barriers above $100\,kJ\,mol^{-1}$, these atropisomers do not isomerise spontaneously at room temperature (*43*, *44*). They were separated by column chromatography, with the *syn*-atropisomer **17** having the smaller retention factor on thin-layer chromatographs. To confirm this empirical assignment, both atropisomers were reacted with heptanoic diacid chloride **18**. The bridged NDI **19** was obtained only for the compound assigned to the *syn*-atropisomer **17**. In the ^{1}H NMR spectrum of macrocycle **19**, the central methylene hydrogens in the middle of the bridge over the π-acidic surface were upfield shifted to 0.25 ppm. They coupled to methylenes at 0.97 ppm, which in turn coupled to the hydrogens in α-position to the carbonyl groups at 1.55 ppm. The *anti*-atropisomer **16** was reacted with 1 equiv. of acetoacetic acid **20**, and the target molecule **12** was isolated from the resulting mixture of diesters, monoesters and unreacted *anti*-diol **16**.

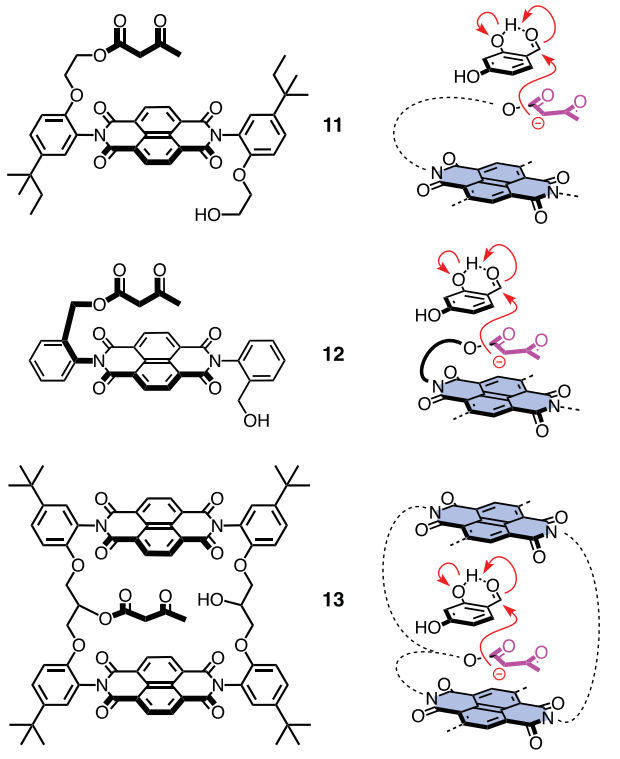

Figure 2. (Colour online) Anion–π systems designed to explore coumarin synthesis on π-acidic surfaces, with schematic indication of their envisioned advantages to stabilise anionic transition states during coumarin synthesis (right, compare Scheme 1).

The macrocyclic anion–π substrate **13** was synthesised from phenol **21** with a solubilising *tert*-butyl group in para-position (Scheme 3). Nitration in ortho-position was followed by reaction of product **22** with (±)-epichlorohydrin **23**. The dinitro product **24** was reduced to diamine **25**. For macrocyclisation, diamine **25** and dianhydride **14** were reacted at high dilution in the presence of base in a microwave reactor. The desired macrocycle **26** containing two NDIs and two secondary alcohols could be isolated in maximal 14% yield. Other components of the quite complex product mixture included the expanded macrocycle with three NDIs. Macrocycle **26** was isolated as a mixture of stereoisomers. Because of the poor performance of the final product (see below), this mixture was not further analysed. Esterification with acetoacetic acid **20** gave the target molecule **13** in 35% yield besides the corresponding diester and unreacted starting material.

Table 1. Kinetic data for coumarin synthesis.[a]

Entry	Cpd[b]	k_{app} ($M^{-1}\,s^{-1}$)[c]	k_{rel}[d]	$\Delta\Delta G_{TS}$ ($kJ\,mol^{-1}$)[e]
1	**3**	$0.30 \pm 0.02 \times 10^{-1}$	–	–
2	**11**	$2.39 \pm 0.07 \times 10^{-1}$	8.0	5.2
3	**12**	$4.55 \pm 0.11 \times 10^{-1}$	15.2	6.7
4	**13**	$0.89 \pm 0.04 \times 10^{-1}$	2.6	2.7

[a] Data for entry 1 and 2 are taken from (*3*).
[b] Compounds, see Figure 2.
[c] Apparent second order rate constant.
[d] Rate enhancement compared to substrate **3**.
[e] Transition-state stabilization compared to substrate **3**.

Consistent with the presence of a mixture of stereoisomers, the acetoacetate part of anion–π substrate **13** appeared in two separate sets of signals in the ^{1}H NMR spectrum. The methyl hydrogens, for example, appeared at $\delta = 2.05$ ppm and $\delta = 1.90$ ppm in a nearly 1:1 ratio, the acidic hydrogens appeared between two carbonyl groups at $\delta = 3.29$ ppm and $\delta = 2.99$ ppm. Compared to the $\delta = 2.25$ and 3.41 ppm for the same hydrogens in the ethyl ester **3**, these upfield shifts demonstrated that the acetoacetates are exposed to the ring current of the NDIs and thus included in the macrocycle. The same hydrogens in anion–π substrate **12** appeared at $\delta = 3.31$ ppm and $\delta = 2.12$ ppm. These comparably weaker upfield shifts of $\Delta\delta \sim -0.11$ suggested that the average location of the acetoacetate should be near the area where the effect of the ring current inverts from shielding to deshielding (*45*), or that contributions from conformers with acetoacetates that are rotated away from the π-surface are quite significant. A more peripheral average location of the acetoacetate was predicted as ideal to preserve enough free space on the π-acidic surface to stabilise the anionic cascade process transforming the acetoacetate into coumarin **1**. For comparison, the firmly fixed hydrogens in the middle of the alkyl bridge over the π-acidic surface of macrocycle **19** showed upfield shifts up to $\delta = 0.25$ ppm, i.e. $\Delta\delta = -1.05$.

Coumarin synthesis is an attractive reaction to probe cascade processes with anion–π interactions because product formation can be easily followed by absorption spectroscopy. In the spectra of the reaction mixture, the maximum of coumarin **1** appeared at $\lambda_{max} = 435$ nm (Figure 3). This red-shifted maximum was clearly separated from the absorption of the NDI in anion–π substrates **12** and **13** at $\lambda_{max} = 379$ nm and the resorcylaldehyde substrate **2** at $\lambda_{max} = 336$ nm. To assure comparability of the results, the kinetic measurements were conducted under conditions used previously for substrates **3** and **11** (*3*). Namely, a 100 mM solution of anion–π substrate **12** in EtOH/$CHCl_3$ 1:1 was incubated with 300 mM resorcylaldehyde **2** and 10 mM piperidine, at room temperature. At appropriate intervals, an aliquot was taken and the absorption spectrum was recorded. The coumarin band at long wavelength increased with increasing reaction time, whereas that of the aldehyde substrate at high energy decreased and that of the NDI in between remained constant, demonstrating that the π-surface is not modified during the reaction. With anion–π substrate **12**, the coumarin absorption at $\lambda_{max} = 435$ nm

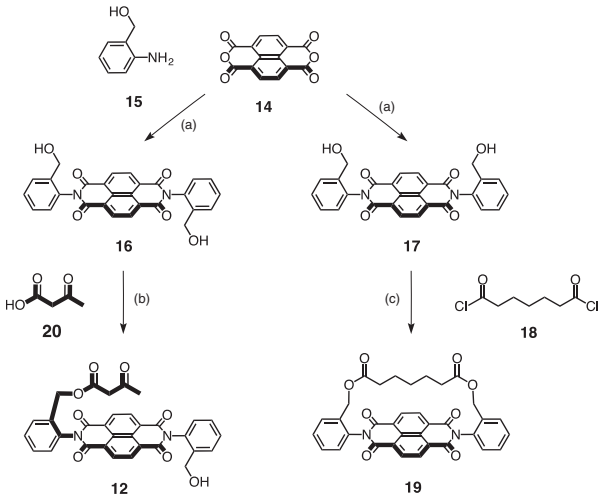

Scheme 2. Synthesis of anion–π substrate **12**. (a) TEA, DMF, 140°C, 10 h, 65% (25% **16**, 40% **17**). (b) EDC, DMAP, TEA, CH_2Cl_2, 0°C to r.t., 14 h, 20%. (c) CH_2Cl_2, TEA, 0°C, 60 min, 31%.

increased clearly faster than with control substrate **3** (Figure 4, □ vs ◆).

From the coumarin absorption, the increase of product concentration with reaction time could be calculated (Figure 4, □). The slope of the obtained plot then gave the initial velocities v_{ini}, which gave an apparent second-order rate constant $k_{app} = 4.55 \times 10^{-5}\,M^{-1}\,s^{-1}$ for **12** (Table 1). A rate enhancement $k_{rel} = 15.2$ was calculated in comparison with the $k_{app} = 3.00 \pm 0.16 \times 10^{-6}\,M^{-1}\,s^{-1}$ obtained for acetoacetate **3** (*3*). From the rate enhancement, a transition-state stabilisation $\Delta\Delta G_{TS} = 6.7$ kJ mol^{-1} relative to coumarin synthesis with acetoacetate **3** was approximated. The same procedure was used to determine rate enhancement and transition-state stabilisation with macrocyclic substrate **13**.

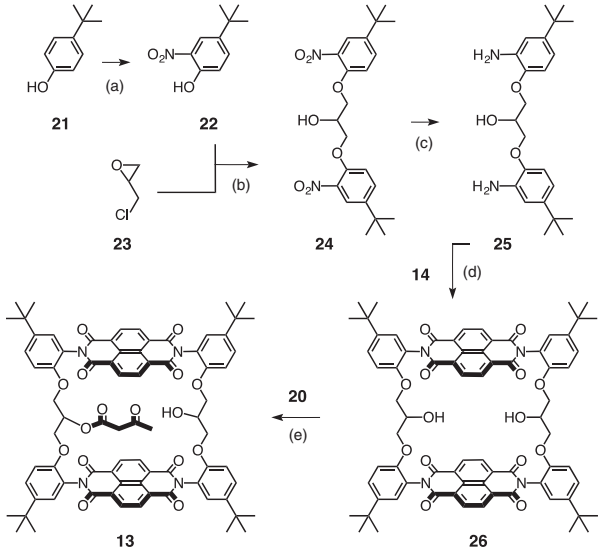

Scheme 3. Synthesis of anion–π substrate **13**. (a) AcOH, HNO_3, 93%. (b) H_2O, NaOH, N_2, 60°C, 25%. (c) H_2, Pd/C, MeOH, r.t., 97%. (d) TEA, DMF, μW, 140°C, 14%. (e) EDC, DMAP, TEA, CH_2Cl_2 0°C to r.t., 14 h, 30%.

Compared to the original π-acidic substrate **11**, rate enhancements with **12** nearly doubled to $k_{rel} = 15.2$ (Table 1). These improvements originated from a more compact structure, with a *pseudo*-Leonard linker intended to place the acetoacetate closer to the π-acidic surface. Consistent with pertinent shifts in the ^{1}H NMR spectra, the shorter linker between π-surface and acetoacetate in **12** was further expected to preserve more free space on the surface to accommodate the anions during the cascade process. The different nature of alcohols used in anion–π substrates **11** and **12** implied that differences in the nature of the leaving group in the last step, the basicity of the enolate stabilised on the π-acidic surface in the first step, etc, could also contribute to the significant increase in activity. However, these differences in the nature of the leaving groups appear too small to cause the observed differences in reactivity. Moreover, the trends should be reversed, **11** (2-methoxyethanol, $pK_a = 14.8$) should be slightly more reactive than **12** (benzylalcohol, $pK_a = 15.4$) (*46*) (Figure 2), which is obviously not the case (Table 1).

The presence of a π-basic pyrene surface in control substrate **27** has been shown previously to have negligible influence on the velocity of coumarin synthesis (Figure 4, X) (*3*). In additional support of operational anion–π interactions, previous studies have also provided unambiguous evidence that covalently positioned enolate bases are stabilised on the same NDI surfaces by $\Delta pK_a = 1.9$ (*3*), anion binding has been demonstrated experimentally (*34*), theoretically (*34*) and in crystal structures (*31*), and the

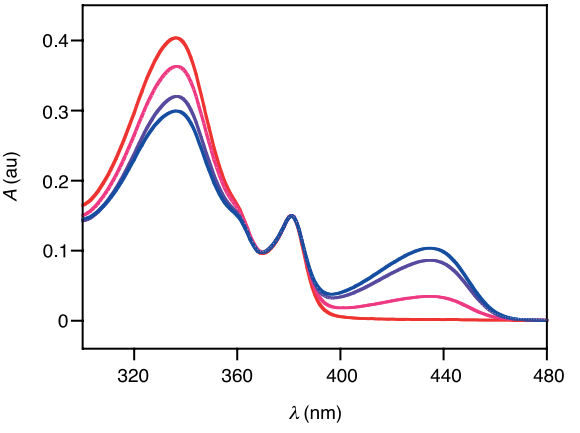

Figure 3. (Colour online) Changes in the absorption spectra during the synthesis of coumarin **1** ($\lambda_{max} = 435$ nm) from aldehyde **2** (300 mM, $\lambda_{max} = 336$ nm), NDI–acetoacetate **12** (100 mM, $\lambda_{max} = 379$ nm) and piperidine (10 mM) in EtOH/$CHCl_3$ 1:1, room temperature. Spectra were taken at 0, 0.9, 3.0 and 4.2 h (with increasing absorption at 435 nm).

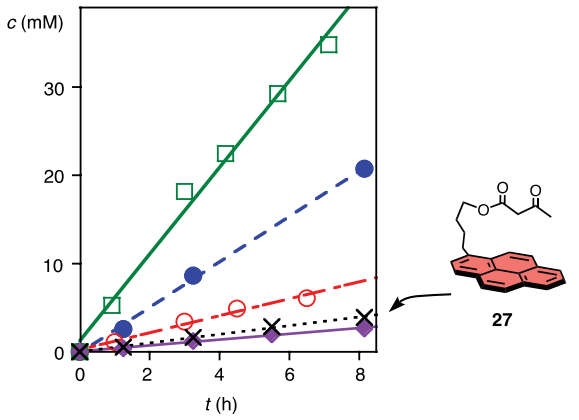

Figure 4. (Colour online) Product concentration c as a function of reaction time t for **3** (◆), **13** (◯), **11** (•), **12** (□) and **27** (X) with linear curve fit. Conditions: 100 mM substrates, 300 mM of **2**, 10 mM piperidine, EtOH/$CHCl_3$ 1:1, room temperature. For changes in absorption, see Figure 3. For data analysis, see Table 1. Data for **3**, **11** and **27** are from (*3*).

role of π–π interactions has been elaborated in the context of nitrate–π recognition (*29*, *33*, *34*).

To further increase the impact of anion–π interactions on coumarin synthesis, either the π-acidity of a monomeric surface or the number of π-surfaces could be increased. Increasing π-acidity of monomeric surfaces has been shown previously to increase the transition-state stabilisation of the Kemp elimination (*1*, *2*). The impact of an increasing number of π-acidic surfaces around the acetoacetate substrate was explored with macrocycle **13**. Clearly slower coumarin synthesis than the operational π-acidic substrates **11** and **12** was found (Figure 4, ◯, Table 1, entry 4). Different reasons can be imagined to explain the disappointing performance of the divalent macrocycle **13**. Various forms of hindered access of base or substrate to the π-surfaces or an enolate anion sandwiched between them would be among the nicest. Too strong anion binding within a π-acidic macrocycle has been evoked previously to account for poor anion transport activity (*34*). Alternative explanations could consider poor solubility, topological mismatches, interference from π–π interactions, leaving group properties (*46*) and so on.

Conclusions

The general objective of this study was to explore the possible acceleration of anionic cascade processes on π-acidic surfaces. The reported results indicate that increasing proximity to single π-acidic NDI surfaces increasingly accelerates coumarin synthesis, whereas inclusion within π-acidic macrocycles decelerates coumarin synthesis. The latter could be explained by steric hindrance and the former by operational anion–π interactions. These possible contributions from anion–π interactions are further supported by the inability of π-basic pyrene surfaces to significantly accelerate coumarin synthesis (*3*), by the stabilisation of enolate anions by $\Delta pK_a = 1.9$ (*3*) together with extensive experimental and theoretical evidence for the recognition, translocation and transformation of various anions on the same NDI surfaces, increasing with increasing π-acidity, and even by crystal structures (*1*, *2*, *31*, *34*). However, further significant efforts will be needed to fully work out the role of anion–π interactions in coumarin synthesis and their ability to catalyse chemical reactions in general. Studies in this direction are ongoing and will be reported in due course.

Supporting information

Experimental details can be found here: http://dx.doi.org/10.1080/10610278.2014.959013

Acknowledgements

We thank the NMR and the Sciences Mass Spectrometry (SMS) platforms for services.

Funding

We thank the University of Geneva, the European Research Council (ERC Advanced Investigator), the National Centre of Competence in Research (NCCR) Chemical Biology and the Swiss NSF for financial support.

References

(1) Zhao, Y.; Domoto, Y.; Orentas, E.; Beuchat, C.; Emery, D.; Mareda, J.; Sakai, N.; Matile, S. *Angew. Chem. Int. Ed.* **2013**, *52*, 9940–9943.
(2) Zhao, Y.; Beuchat, C.; Mareda, J.; Domoto, Y.; Gajewy, J.; Wilson, A.; Sakai, N.; Matile, S. *J. Am. Chem. Soc.* **2014**, *136*, 2101–2111.
(3) Zhao, Y.; Sakai, N.; Matile, S. *Nat. Commun.* **2014**, *5*, 3911.
(4) Shepodd, T.J.; Petti, M.A.; Dougherty, D.A. *J. Am. Chem. Soc.* **1988**, *110*, 1983–1985.
(5) Dougherty, D.A. *Acc. Chem. Res.* **2013**, *46*, 885–893.
(6) Wendt, K.U.; Schulz, G.E.; Corey, E.J.; Liu, D.R. *Angew. Chem. Int. Ed.* **2000**, *39*, 2812–2833.
(7) Knowles, R.R.; Lin, S.; Jacobsen, E.N. *J. Am. Chem. Soc.* **2010**, *132*, 5030–5032.
(8) Yamada, S.; Fossey, J.S. *Org. Biomol. Chem.* **2011**, *9*, 7275–7281.
(9) Quinonero, D.; Garau, C.; Rotger, C.; Frontera, A.; Ballester, P.; Costa, A.; Deya, P.M. *Angew. Chem. Int. Ed.* **2002**, *41*, 3389–3392.
(10) Mascal, M.; Armstrong, A.; Bartberger, M.D. *J. Am. Chem. Soc.* **2002**, *124*, 6274–6276.
(11) Alkorta, I.; Rozas, I.; Elguero, J. *J. Am. Chem. Soc.* **2002**, *124*, 8593–8598.
(12) Chifotides, H.T.; Dunbar, K.R. *Acc. Chem. Res.* **2013**, *46*, 894–906.

(13) Frontera, A.; Gamez, P.; Mascal, M.; Mooibroek, T.J.; Reedijk, J. *Angew. Chem. Int. Ed.* **2011**, *50*, 9564–9583.
(14) Watt, M.M.; Collins, M.S.; Johnson, D.W. *Acc. Chem. Res.* **2013**, *46*, 955–966.
(15) Wheeler, S.E. *Acc. Chem. Res.* **2013**, *46*, 1029–1038.
(16) Wheeler, S.E.; Houk, K.N. *J. Phys. Chem. A* **2010**, *114*, 8658–8664.
(17) Hay, B.P.; Custelcean, R. *Cryst. Growth Des.* **2009**, *9*, 2539–2545.
(18) Guha, S.; Goodson, F.S.; Corson, L.J.; Saha, S. *J. Am. Chem. Soc.* **2012**, *134*, 13679–13691.
(19) Schwans, J.P.; Sunden, F.; Lassila, J.K.; Gonzalez, A.; Tsai, Y.; Herschlag, D. *Proc. Natl. Acad. Sci. USA* **2013**, *110*, 11308–11313.
(20) Bauzá, A.; Quiñonero, D.; Deyà, P.M.; Frontera, A. *Chem. Eur. J.* **2014**, *20*, 6985–6990.
(21) Salonen, L.M.; Ellermann, M.; Diederich, F. *Angew. Chem. Int. Ed.* **2011**, *50*, 4808–4842.
(22) Schneider, H.-J. *Acc. Chem. Res.* **2013**, *46*, 1010–1019.
(23) Giese, M.; Albrecht, M.; Krappitz, T.; Peter, M.; Gossen, V.; Raabe, G.; Valkonen, A.; Rissanen, K. *Chem. Commun.* **2012**, *48*, 9983–9985.
(24) Cadman, C.J.; Croft, A.K. *Beilstein J. Org. Chem.* **2011**, *7*, 320–328.
(25) Rosokha, Y.S.; Lindeman, S.V.; Rosokha, S.V.; Kochi, J.K. *Angew. Chem. Int. Ed.* **2004**, *43*, 4650–4652.
(26) Maeda, H.; Morimoto, T.; Osuka, A.; Furuta, H. *Chem. Asian J.* **2006**, *1*, 832–844.
(27) Wang, D.-X.; Zheng, Q.Y.; Wang, Q.Q.; Wang, M.-X. *Angew. Chem. Int. Ed.* **2008**, *47*, 7485–7488.
(28) Chudzinski, M.G.; McClary, C.A.; Taylor, M.S. *J. Am. Chem. Soc.* **2011**, *133*, 10559–10567.
(29) Watt, M.M.; Zakharov, L.N.; Haley, M.M.; Johnson, D.W. *Angew. Chem. Int. Ed.* **2013**, *52*, 10275–10280.
(30) Wang, D.-X.; Wang, M.-X. *J. Am. Chem. Soc.* **2013**, *135*, 892–897.
(31) Schneebeli, S.T.; Frasconi, M.; Liu, Z.; Wu, Y.; Gardner, D. M.; Strutt, N.L.; Cheng, C.; Carmieli, R.; Wasielewski, M. R.; Stoddart, J.F. *Angew. Chem. Int. Ed.* **2013**, *52*, 13100–13104.
(32) Ballester, P. *Acc. Chem. Res.* **2013**, *46*, 874–884.
(33) Adriaenssens, L.; Estarellas, C.; Vargas Jentzsch, A.; Martinez Belmonte, M.; Matile, S.; Ballester, P. *J. Am. Chem. Soc.* **2013**, *135*, 8324–8330.
(34) Dawson, R.E.; Hennig, A.; Weimann, D.P.; Emery, D.; Ravikumar, V.; Montenegro, J.; Takeuchi, T.; Gabutti, S.; Mayor, M.; Mareda, J.; Schalley, C.A.; Matile, S. *Nat. Chem.* **2010**, *2*, 533–538.
(35) Vargas Jentzsch, A.; Emery, D.; Mareda, J.; Metrangolo, P.; Resnati, G.; Matile, S. *Angew. Chem. Int. Ed.* **2011**, *50*, 11675–11678.
(36) Barton, D.; Nakanishi, K.; Meth-Cohen, O.; Eds. *Comprehensive Natural Products Chemistry*; Oxford: Elsevier Science Ltd, 1999.
(37) Cane, D.E.; Walsh, C.T.; Khosla, C. *Science* **1998**, *282*, 63–68.
(38) Jenni, S.; Leibundgut, M.; Boehringer, D.; Frick, C.; Mikolásek, B.; Ban, N. *Science* **2007**, *316*, 254–261.
(39) Walker, M.C.; Thuronyi, B.W.; Charkoudian, L.K.; Lowry, B.; Khosla, C.; Chang, M.C. *Science* **2013**, *341*, 1089–1094.
(40) Bretschneider, T.; Heim, J.B.; Heine, D.; Winkler, R.; Busch, B.; Kusebauch, B.; Stehle, T.; Zocher, G.; Hertweck, C. *Nature* **2013**, *502*, 124–128.
(41) Bernardi, L.; Fochi, M.; Franchini, C.M.; Ricci, A. *Org. Biomol. Chem.* **2012**, *10*, 2911–2922.
(42) Lubkoll, J.; Wennemers, H. *Angew. Chem. Int. Ed.* **2007**, *46*, 6841–6844.
(43) Lavin, J.M.; Shimizu, K.D. *Org. Lett.* **2006**, *8*, 2389–2392.
(44) Shimizu, K.D.; Dewey, T.M.; Rebek, Jr., J. *J. Am. Chem. Soc.* **1994**, *116*, 5145–5149.
(45) Haigh, C.W.; Mallion, R.B. *Org. Magn. Reson.* **1972**, *4*, 203–228.
(46) Murto, J. *Acta Chem. Scand.* **1964**, *18*, 1043–1053.